Imaging of Human Epidermal Growth Factor Receptor Type 2 Expression with ^{18}F-Labeled Affibody Molecule $Z_{HER2:2395}$ in a Mouse Model for Ovarian Cancer

Sandra Heskamp[1,2], Peter Laverman[2], Daniel Rosik[3], Frederic Boschetti[4], Winette T.A. van der Graaf[1], Wim J.G. Oyen[2], Hanneke W.M. van Laarhoven[1], Vladimir Tolmachev[5], and Otto C. Boerman[2]

[1]Department of Medical Oncology, Radboud University Nijmegen Medical Centre, Nijmegen, The Netherlands; [2]Department of Nuclear Medicine, Radboud University Nijmegen Medical Centre, Nijmegen, The Netherlands; [3]Division of Molecular Biotechnology, School of Biotechnology, KTH Royal Institute of Technology, Stockholm, Sweden; [4]CheMatech, Dijon, France; and [5]Division of Biomedical Radiation Sciences, Rudbeck Laboratory, Uppsala University, Uppsala, Sweden

Affibody molecules are small (7 kDa) proteins with subnanomolar targeting affinity. Previous SPECT studies in xenografts have shown that the Affibody molecule ^{111}In-DOTA-$Z_{HER2:2395}$ can discriminate between high and low human epidermal growth factor receptor type 2 (*HER2*)–expressing tumors, indicating that radiolabeled Affibody molecules have potential for patient selection for *HER2*-targeted therapy. Compared with SPECT, PET with positron-emitting radionuclides, such as ^{18}F, may improve imaging of *HER2* expression because of higher sensitivity and improved quantification of PET. The aim of the present study was to determine whether the ^{18}F-labeled NOTA-conjugated Affibody molecule $Z_{HER2:2395}$ is a suitable agent for imaging of *HER2* expression. The tumor-targeting properties of ^{18}F-labeled $Z_{HER2:2395}$ were compared with ^{111}In- and ^{68}Ga-labeled $Z_{HER2:2395}$ in mice with *HER2*-expressing SK-OV-3 xenografts. **Methods:** $Z_{HER2:2395}$ was conjugated with NOTA and radiolabeled with ^{18}F, ^{68}Ga, and ^{111}In. Radiolabeling with ^{18}F was based on the complexation of Al^{18}F by NOTA. The 50% inhibitory concentration values for NOTA-$Z_{HER2:2395}$ labeled with ^{19}F, ^{69}Ga, and ^{115}In were determined in a competitive cell-binding assay using SK-OV-3 cells. Mice bearing subcutaneous SK-OV-3 xenografts were injected intravenously with radiolabeled NOTA-$Z_{HER2:2395}$. One and 4 h after injection, PET/CT or SPECT/CT images were acquired, and the biodistribution was determined by ex vivo measurement. **Results:** The 50% inhibitory concentration values for ^{19}F-, ^{69}Ga-, and ^{115}In-NOTA-$Z_{HER2:2395}$ were 5.0, 6.3, and 5.3 nM, respectively. One hour after injection, tumor uptake was 4.4 ± 0.8 percentage injected dose per gram (%ID/g), 5.6 ± 1.6 %ID/g, and 7.1 ± 1.4 %ID/g for ^{18}F-, ^{68}Ga-, and ^{111}In-NOTA-$Z_{HER2:2395}$, respectively, and the respective tumor-to-blood ratios were 7.4 ± 1.8, 8.0 ± 1.3, and 4.8 ± 1.3. Tumor uptake was specific, because uptake could be blocked efficiently by coinjection of an excess of unlabeled $Z_{HER2:2395}$. PET/CT and SPECT/CT images clearly visualized *HER2*-expressing SK-OV-3 xenografts. **Conclusion:** This study showed that ^{18}F-NOTA-$Z_{HER2:2395}$ is a promising new imaging agent for *HER2* expression in tumors. Affibody molecules were successfully labeled with ^{18}F within 30 min, based on the complexation of Al^{18}F by NOTA. Further research is needed to determine whether this technique can be used for patient selection for *HER2*-targeted therapy.

Key Words: *HER2*; Affibody molecule; PET; ^{18}F; ovarian cancer

J Nucl Med 2012; 53:146–153
DOI: 10.2967/jnumed.111.093047

Human epidermal growth factor receptor 2 (*HER2*) is a member of the epidermal growth factor receptor family. Dimerization of *HER2* with other members of the epidermal growth factor receptor family leads to activation of several downstream pathways, including PI3K-AKT and MAPK, resulting in increased tumor cell proliferation, cell motility, and survival (*1*). *HER2* is overexpressed in 18%–25% of all breast carcinomas and in subsets of ovarian, lung, prostate, and gastric cancers (*1,2*). Breast cancers that overexpress *HER2* have been associated with aggressive tumor growth, high relapse, and poor prognosis (*2*). Furthermore, *HER2*-overexpressing tumors may be more resistant to endocrine therapy and chemotherapy (*3*).

Different therapeutic strategies have been developed to target *HER2*, including the monoclonal antibody trastuzumab and tyrosine kinase inhibitor lapatinib. Trastuzumab targets the extracellular domain of *HER2*, inhibits intracellular signaling pathways, and causes antibody-dependent cell-mediated cytotoxicity (*1*). Trastuzumab significantly improves survival of patients with *HER2*-positive advanced breast and gastric cancer, when combined with chemotherapy(*4–6*). Lapatinib targets the intracellular domain of both *HER2* and epidermal growth factor receptor (*1*). The addition of lapatinib to capecitabine prolongs progression-free survival of patients with advanced *HER2*-positive breast cancer (*7*).

Received May 13, 2011; revision accepted Aug. 30, 2011.
For correspondence or reprints contact: Sandra Heskamp, Radboud University Nijmegen Medical Centre, Department of Nuclear Medicine (Internal Postal Code 756), P.O. Box 9101, 6500 HB Nijmegen, The Netherlands.
E-mail: s.heskamp@nucmed.umcn.nl
Published online Dec. 15, 2011.

Currently, trastuzumab treatment is recommended only for breast and gastric cancer patients with *HER2*-overexpressing tumors (*8*). Therefore, accurate assessment of *HER2* expression is essential for patient selection for *HER2*-targeted therapy. Nowadays, *HER2* expression is determined on tumor biopsies by immunohistochemical staining of *HER2* protein expression or fluorescence in situ hybridization of *HER2* messenger RNA expression. Up to 20% of the current *HER2* assessments may be inaccurate (*9,10*). Furthermore, *HER2* expression can differ between the primary tumor and metastases (*11,12*). Therefore, in vivo imaging of *HER2* expression may result in more accurate detection of *HER2* expression, avoiding misinterpretation due to intratumoral and interlesional heterogeneity. Moreover, such an imaging method would allow monitoring of *HER2* expression during the course of disease, without the need of repetitive invasive biopsies.

Several approaches have been used for PET and SPECT of *HER2* expression, including radiolabeled antibodies trastuzumab and pertuzumab (*HER2* dimerization inhibitor) and radiolabeled trastuzumab fragments (*13–16*). These radiotracers were able to visualize *HER2* expression, but their large size resulted in slow tumor accumulation and slow clearance from the circulation. A new class of targeting proteins are Affibody (Affibody AB) molecules. These are based on a 58-amino-acid (7 kDa) scaffold and can be selected to bind with high affinity to various tumor-associated antigens. Their small size allows rapid extravasation in tumors and rapid clearance from the blood, resulting in high-contrast imaging within several hours after injection (*17,18*). The *HER2*-targeting Affibody molecule $Z_{HER2:342}$ and its derivates have been radiolabeled with several radionuclides and have shown specific targeting of *HER2* (*17*). Previous studies in xenografts have shown that the Affibody molecule ^{111}In-DOTA-$Z_{HER2:2395}$ can discriminate between tumors with high and low *HER2* expression (*19*). A clinical pilot study with ^{111}In- and ^{68}Ga-DOTA-$Z_{HER2:342}$ has shown that it is feasible to visualize *HER2*-expressing tumors in patients with metastatic breast cancer (*20*). Therefore, Affibody molecules have the potential for patient selection for *HER2*-targeted therapy.

Recently, $Z_{HER2:2395}$, a variant of $Z_{HER2:342}$ with a C-terminal cysteine, was coupled to maleimide monoamide NOTA (MMA-NOTA) and was radiolabeled with ^{111}In. This site-specifically labeled conjugate allowed high-contrast imaging of *HER2*-expressing xenografts (*21*). Imaging of *HER2* expression with Affibody molecules can be improved by the use positron-emitting radionuclides such as ^{18}F, because of the higher sensitivity and better quantification of PET than SPECT. Kramer-Marek et al. have conjugated $Z_{HER2:342}$ with *N*-2-(4-^{18}F-fluorobenzamido)ethyl] maleimide (^{18}F-FBEM) (*22*). ^{18}F-FBEM-$Z_{HER2:342}$ could visualize *HER2*-expressing tumors. However, this labeling reaction required a long synthesis time. Lately, a new method was described for labeling of NOTA-conjugated peptides with ^{18}F, which is based on the formation of aluminum^{18}F-fluoride (Al^{18}F) and its complexation by NOTA (*23,24*). This method allows rapid and efficient labeling of peptides and proteins with ^{18}F.

The aim of the present study was to determine whether the ^{18}F-labeled Affibody molecule $Z_{HER2:2395}$ is a suitable imaging agent for *HER2* expression in mice with SK-OV-3 xenografts. For this purpose, NOTA-conjugated $Z_{HER2:2395}$ was radiolabeled with ^{18}F, based on the complexation of Al^{18}F by NOTA. ^{18}F-NOTA-$Z_{HER2:2395}$ was compared with ^{111}In- and ^{68}Ga-labeled $Z_{HER2:2395}$.

MATERIALS AND METHODS

Cell Line and Affibody Molecule

The *HER2*-overexpressing ovarian cancer cell line SK-OV-3 was cultured and maintained as a monolayer in RPMI 1640 medium (Gibco, BRL Life Sciences Technologies) supplemented with 10% fetal calf serum, 2 mM glutamine, penicillin (100 units/mL), and streptomycin (100 μg/mL). The *HER2*-negative breast cancer cell line SUM149 (Asterand) was cultured and maintained as monolayer in Ham F12 medium (Gibco, BRL Life Sciences Technologies) supplemented with 5% fetal calf serum, 10 mM *N*-(2-hydroxyethyl)piperazine-*N*′-(2-ethanesulfonic acid) (HEPES), hydrocortisone (1 μg/mL), and insulin (5 μg/mL) at 37° C in a humidified atmosphere with 5% CO_2. $Z_{HER2:2395}$ was produced as described previously (*25*).

Affibody Conjugation with MMA-NOTA

The production of MMA-NOTA and coupling of MMA-NOTA to $Z_{HER2:2395}$ has been described elsewhere (*21,25*). In short, reduced $Z_{HER2:2395}$ was incubated for 1 h at 37°C with a freshly prepared solution of MMA-NOTA in 0.2 M ammonium acetate, pH 5.5 (1 mg/mL), at a chelator-to-protein ratio of 3:1. The NOTA-conjugated Affibody molecules were purified by semipreparative reversed-phase high-performance liquid chromatography (HPLC), using a 300SB C18 column (9.4 × 250 mm; Zorbax) at a flow rate of 8 mL/min, with the following buffer system: buffer A, 0.1% trifluoroacetic acid (TFA) in water; buffer B, 0.1% TFA in acetonitrile; and a gradient of 25%–40% buffer B over 11 min.

Radiolabeling

^{18}F Labeling. Radiolabeling with ^{18}F was based on the complexation of Al^{18}F by NOTA as described elsewhere (*23*,*24*). Briefly, a Chromafix PS-HCO_3 cartridge (ABX) with 2–6 GBq of ^{18}F (BV Cyclotron VU) was washed with 3 mL of metal-free water. ^{18}F was eluted from the cartridge with 100 μL of 0.9% NaCl. Al^{18}F was prepared by adding 2 mM $AlCl_3$ in 0.1 M sodium acetate, pH 4 (8.5 μL of $AlCl_3$ per GBq of ^{18}F). NOTA-$Z_{HER2:2395}$ (250 μg) was dissolved in 25 μL of 0.5 M sodium acetate, pH 4. To the dissolved Affibody molecule, 25 μL of acetonitrile were added. After adding 50 μL of Al^{18}F (1.16–1.27 GBq), the reaction mixture was incubated for 15 min at 90°C. Subsequently, the reaction mixture was applied on a 1-mL Oasis HLB cartridge (30 mg; Waters) to remove unincorporated Al^{18}F. The cartridge was washed with 3 mL of H_2O, and ^{18}F-NOTA-$Z_{HER2:2395}$ was eluted with 300 μL of ethanol. Finally, ^{18}F-NOTA-$Z_{HER2:2395}$ was applied on a NAP-5 column (GE Healthcare Life Sciences), preequilibrated with phosphate-buffered saline (PBS), to change the buffer from ethanol to PBS. Before injection, ^{18}F-NOTA-$Z_{HER2:2395}$ was diluted in PBS containing 0.5% bovine serum albumin (BSA). Labeling efficiency and radio-

chemical purity were determined with instant-thin layer chromatography (ITLC) and HPLC.

^{68}Ga Labeling. NOTA-$Z_{HER2:2395}$ was labeled with ^{68}Ga eluted from a TiO_2-based 1,850-MBq ^{68}Ge/^{68}Ga generator (IGG-100; Eckert and Ziegler) using 0.1 M HCl (Ultrapure; J.T. Baker). NOTA-$Z_{HER2:2395}$ was dissolved in 0.25 M ammonium acetate, pH 5.4. Radiolabeling with ^{68}Ga was performed by adding 120 μL of 2.5 M HEPES, pH 5.6, and 1 mL of ^{68}Ga eluate (165–192 MBq) to NOTA-$Z_{HER2:2395}$ (18–21 μg). The final pH of the labeling reaction was 3.5. The reaction mixture was incubated for 15 min at 90°C. After the labeling reaction, 50 mM ethylenediaminetetraacetic acid (EDTA) was added to a final concentration of 5 mM to complex nonincorporated $^{68}Ga^{3+}$. Subsequently, the labeling mixture was purified on a PD10 column (GE Healthcare Life Sciences), eluted with PBS containing 0.5% BSA. Before injection, ^{68}Ga-NOTA-$Z_{HER2:2395}$ was diluted in PBS containing 0.5% BSA. Labeling efficiency, colloid, and radiochemical purity were determined with ITLC and HPLC.

^{111}In Labeling. NOTA-$Z_{HER2:2395}$ was dissolved in 0.25 M ammonium acetate, pH 5.4. For radiolabeling, 70 μg of NOTA-$Z_{HER2:2395}$ was incubated with 260 MBq of ^{111}In (Covidien BV) in 0.1 M 2-(*N*-morpholino)ethanesulfonic acid buffer, pH 5.4 (twice the volume of ^{111}In), for 15 min at 90°C. After incubation, 50 mM EDTA was added to a final concentration of 5 mM. Subsequently, the reaction mixture was purified on a PD10 column, eluted with PBS containing 0.5% BSA. ^{111}In-NOTA-$Z_{HER2:2395}$ was diluted in PBS containing 0.5% BSA. Labeling efficiency and radiochemical purity were determined with ITLC and HPLC.

Quality Control

HPLC. Labeling efficiency was analyzed by reversed-phase high-performance liquid chromatography on an Agilent 1200 system (Agilent Technologies). A monolithic C18 column (Onyx, 4.6 × 100 mm; Phenomenex) was used at a flow rate of 1 mL/min, with the following buffer system: buffer A, 0.1% v/v TFA in water; buffer B, 0.1% v/v TFA in acetonitrile; and a gradient of 97% buffer A to 0% buffer A at 5–15 min. The radioactivity of the eluate was monitored using an in-line NaI radiodetector (Raytest GmbH). Elution profiles were analyzed using Gina-star software (version 2.18; Raytest GmbH).

ITLC. Radiochemical purity was determined using ITLC on silica gel chromatography strips (Agilent Technologies), with 0.1 M ammonium acetate containing 0.1 M EDTA, pH 5.5, as the mobile phase. The presence of colloid was analyzed using methanol:0.5 M HEPES, pH 3.5 (1:1) as the mobile phase.

In Vitro Studies

In Vitro Binding of Radiolabeled NOTA-$Z_{HER2:2395}$. Labeling with ^{18}F requires incubation of the NOTA-conjugated Affibody molecule at 90°C in 25% acetonitrile. To determine whether *HER2* binding was affected by these labeling conditions, an in vitro binding experiment was performed. NOTA-$Z_{HER2:2395}$ was radiolabeled with ^{18}F. Unlabeled NOTA-$Z_{HER2:2395}$ was incubated for 15 min at room temperature without acetonitrile or at 90°C in the presence of 25% acetonitrile.

SK-OV-3 and SUM149 cells were cultured to confluency in 6-well plates. Cells were washed with PBS and incubated for 2 h at 4°C with 4 kBq of ^{18}F-NOTA-$Z_{HER2:2395}$, without unlabeled Affibody molecules or in the presence of 50 nM unlabeled NOTA-$Z_{HER2:2395}$ (preincubated at room temperature or 90°C) in a total volume of 1 mL of binding buffer (SK-OV-3: RPMI 1640 containing 0.5% BSA; SUM149: Ham F12, 10 mM HEPES, containing 0.5% BSA). Separate wells were incubated with 4 kBq of ^{18}F-NOTA-$Z_{HER2:2395}$ and 50 nM trastuzumab to study whether trastuzumab interfered with Affibody molecule binding. After incubation, cells were washed with PBS, and the cell-associated activity was measured in a shielded well-type γ-counter (Perkin-Elmer).

Scatchard Analysis. Scatchard analysis was performed to determine the dissociation constant (K_d) and the number of binding sites for ^{18}F-NOTA-$Z_{HER2:2395}$ on SK-OV-3 cells. Cells were cultured to confluency in 6-well plates and were incubated for 2 h at 4°C with increasing concentrations of ^{18}F-NOTA-$Z_{HER2:2395}$ (0.03–30 nM) in 1 mL of binding buffer. Nonspecific binding was determined by coincubation with an excess of 1 μM unlabeled NOTA-$Z_{HER2:2395}$. After incubation, cells were washed with PBS, and the cell-associated activity was measured in a shielded well-type γ-counter.

50% Inhibitory Concentration (IC_{50}) Determination. The IC_{50} for binding *HER2* on SK-OV-3 was determined in a competitive binding assay using ^{19}F-, ^{69}Ga-, or ^{115}In-NOTA-$Z_{HER2:2395}$ to compete for binding with ^{111}In-NOTA-$Z_{HER2:2395}$.

NOTA-$Z_{HER2:2395}$ was dissolved in 0.25 M ammonium acetate, pH 5.4. ^{19}F-NOTA-$Z_{HER2:2395}$ was prepared by adding a 2.5-fold molar excess of $AlCl_3$ and a 5-fold molar excess of ^{19}F to 15 μg of NOTA-$Z_{HER2:2395}$ in 0.5 M sodium acetate, pH 4. ^{115}In-NOTA-$Z_{HER2:2395}$ was prepared by adding a 3-fold molar excess of $^{115}InCl_3$ to 15 μg of NOTA-$Z_{HER2:2395}$ in 0.1 M 2-(*N*-morpholino)ethanesulfonic acid buffer, pH 5.4. ^{69}Ga-NOTA-$Z_{HER2:2395}$ was formed by adding a 3-fold molar excess of ^{69}Ga nitrate to 15 μg of NOTA-$Z_{HER2:2395}$ in 2.5 M HEPES buffer, pH 7.0. All labeling mixtures were incubated for 15 min at 90°C. EDTA (50 mM) was added to a final concentration of 5 mM.

NOTA-$Z_{HER2:2395}$ (10 μg) was radiolabeled with 1.9 MBq of ^{111}In. Labeling efficiency, determined using ITLC, was 95%, and no further purification was required.

SK-OV-3 cells were cultured to confluency in 6-well plates. To determine the apparent IC_{50}, cells were washed with PBS and incubated for 2 h at 4°C in 2 mL of binding buffer with a trace amount of 1 kBq of ^{111}In-NOTA-$Z_{HER2:2395}$ and increasing concentrations of ^{19}F-, ^{69}Ga-, or ^{115}In-NOTA-$Z_{HER2:2395}$ (0.001–30 nM). After incubation, cells were washed with PBS, and the cell-associated activity was measured in a γ-counter. The IC_{50} was defined as the Affibody molecule concentration at which 50% of binding without competitor was reached. IC_{50} values were calculated using Prism software (version 5.03 for Windows [Microsoft]; GraphPad Software).

Serum Stability. ^{18}F-NOTA-$ZHER_{2:2395}$ (3.7 MBq) was incubated for 4 h at 37°C in 500 μL of human and mouse serum. After incubation, stability was analyzed using ITLC.

Animal Studies

Animal experiments were performed in female BALB/c nude mice (Janvier SAS) and were conducted in accordance with the principles laid out by the revised Dutch Act on Animal Experimentation (1997) and approved by the institutional Animal Welfare Committee of the Radboud University Nijmegen. At 6–8 wk of age, mice were inoculated subcutaneously with 5×10^6 SK-OV-3 cells (mixed 2:1 with Matrigel [BD Biosciences]). Experiments were initiated when the tumors reached approximately 0.1 cm^3.

Biodistribution Studies. Five groups ($n = 6$) of mice were injected intravenously with 10 μg of ^{18}F-NOTA-$Z_{HER2:2395}$

(1 MBq), ^{68}Ga-NOTA-$Z_{HER2:2395}$ (5 MBq), or ^{111}In-NOTA-$Z_{HER2:2395}$ (0.4 MBq). Separate groups (n = 3) of mice were coinjected with an excess of unlabeled $Z_{HER2:2395}$ (500 μg). One and 4 h (^{18}F and ^{111}In only) after injection, mice were euthanized by CO_2/O_2 asphyxiation. Tumor, blood, muscle, lung, heart, spleen, pancreas, intestine, kidney, liver, small intestine, and bone were dissected and weighed. Activity was measured in a γ-counter. To calculate the uptake of radiolabeled Affibody molecules in each sample as a fraction of the injected dose, aliquots of the injected dose were counted simultaneously. The results were expressed as percentage of the injected dose per gram (%ID/g).

PET/CT. Mice were injected intravenously with 10 μg of ^{18}F-NOTA-$Z_{HER2:2395}$ (10 MBq) or 10 μg of ^{68}Ga-NOTA-$Z_{HER2:2395}$ (11 MBq). One and 4 h (^{18}F only) after injection, mice were scanned on an animal PET/CT scanner (Inveon; Siemens Preclinical Solutions) with an intrinsic spatial resolution of 1.5 mm (*26*). First, a CT scan (spatial resolution, 113 μm; 80 kV; 500 μA) was acquired for anatomic reference, followed by a PET emission scan of 30 min (1 h after injection) or 60 min (4 h after injection). Before the last scan, mice were euthanized, and after acquisition the biodistribution of radiolabeled Affibody molecules was measured ex vivo. Scans were reconstructed with Inveon Acquisition Workplace software (version 1.5; Siemens Preclinical Solutions), using an ordered-set expectation maximization 3-dimensional maximum a posteriori algorithm with the following parameters: matrix, 256 × 256 × 159; pixel size, 0.43 × 0.43 × 0.8 mm; and β-value of 1.5 with uniform variance. Representative cross sections located approximately in the center of the tumor were displayed. Tumor-to-liver ratios were calculated with the Inveon Research Workplace software (IRW, version 3.0).

SPECT/CT. Mice were injected with 10 μg of ^{111}In-NOTA-$Z_{HER2:2395}$ (18 MBq). One and 4 h after injection, mice were scanned on an animal SPECT/CT device (U-SPECT-II; MILabs), using a 1.0-mm-diameter pinhole rat collimator cylinder (*27*). SPECT scans were acquired for 45 min (1 h after injection) or 60 min (4 h after injection), followed by CT scans (spatial resolution, 160 μm; 40 kV; 612 μA) for anatomic reference. Before the last scan, mice were euthanized, and after acquisition the biodistribution of radiolabeled Affibody molecules was measured ex vivo. Scans were reconstructed with MILabs reconstruction software, which uses an ordered-subset expectation maximization algorithm, with a voxel size of 0.375 mm. Tumor-to-liver ratios were calculated with the Inveon Research Workplace software (IRW, version 3.0).

Statistical Analysis

Statistical analyses were performed using SPSS software (version 16.0) and GraphPad Prism (version 5.03) for Windows. Differences in uptake of radiolabeled Affibody molecules were tested for significance using the nonparametric Mann–Whitney test. A P value below 0.05 was considered significant.

RESULTS

Radiolabeling

The radiolabeling yield for ^{18}F, ^{68}Ga, and ^{111}In was 21.0% ± 5.7%, 84.6% ± 0.9%, and 94.0%, respectively. After purification on an HLB cartridge and NAP-5 column (^{18}F) or PD10 column (^{68}Ga and ^{111}In), ITLC indicated that radiochemical purity exceeded 95%. No colloid (<1%) was formed during the labeling reactions. Specific activities of 7,700 ± 3,000, 39,600 ± 500, and 22,400 GBq/mmol were obtained for ^{18}F-, ^{68}Ga-, and ^{111}In-NOTA-$Z_{HER2:2395}$, respectively (end of synthesis).

In Vitro Binding Assays

In vitro binding assays showed that incubation at 90°C in 25% acetonitrile did not affect binding of NOTA-$Z_{HER2:2395}$ to *HER2* (Fig. 1). Both samples (preincubated at room temperature and 90°C in acetonitrile) were equally effective in blocking the binding of ^{18}F-NOTA-$Z_{HER2:2395}$. Furthermore, ^{18}F-NOTA-$Z_{HER2:2395}$ did not show specific binding to the *HER2*-negative cell line SUM149, and in agreement with previous studies, trastuzumab did not interfere with Affibody molecule binding to SK-OV-3 cells.

Scatchard analysis revealed that the K_d of ^{18}F-NOTA-$Z_{HER2:2395}$ was 6.5 ± 1.2 nM, and the number of binding sites on SK-OV-3 cells was $1.3 \times 10^6 \pm 0.4 \times 10^6$ per cell. The binding curves of the IC_{50} determination are shown in Figure 2. The IC_{50} of ^{19}F-NOTA-$Z_{HER2:2395}$ was 5.0 ± 0.1 nM, which was similar to ^{69}Ga- and ^{115}In-NOTA-$Z_{HER2:2395}$ (6.3 ± 0.1 nM and 5.1 ± 0.04 nM, respectively).

Stability studies showed that ^{18}F-NOTA-$Z_{HER2:2395}$ did not release Al^{18}F after incubation in human or mouse serum at 37°C for 4 h, indicating excellent stability.

Biodistribution Studies

The results of the biodistribution studies are summarized in Figure 3. Mean tumor weight was 112 ± 54 mg. Tumor uptake at 1 h after injection of ^{18}F-NOTA-$Z_{HER2:2395}$ was 4.4% ± 0.8 %ID/g, compared with 5.6% ± 1.6 %ID/g and 7.1% ± 1.4 %ID/g for ^{68}Ga- and ^{111}In-NOTA-$Z_{HER2:2395}$, respectively. Coinjection of an excess of unlabeled $Z_{HER2:2395}$ resulted in a significant ($P < 0.05$) reduction in tumor uptake to 2.9% ± 0.3 %ID/g, 1.7% ± 0.5 % ID/g, and 3.0% ± 0.5 %ID/g for ^{18}F-, ^{68}Ga-, and ^{111}In-NOTA-$Z_{HER2:2395}$, respectively. Uptake in other organs was not affected by the coinjection of an excess of unla-

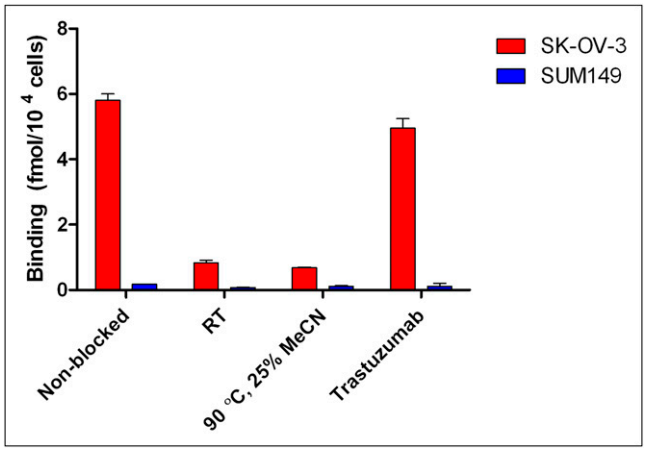

FIGURE 1. In vitro binding of ^{18}F-NOTA-$Z_{HER2:2395}$ to SK-OV-3 and SUM149 cells. Cells were incubated with ^{18}F-NOTA-$Z_{HER2:2395}$ in presence of unlabeled NOTA-$Z_{HER2:2395}$, which was preincubated for 15 min at room temperature without acetonitrile, at 90°C in 25% acetonitrile (MeCN), or in presence of trastuzumab. RT = room temperature.

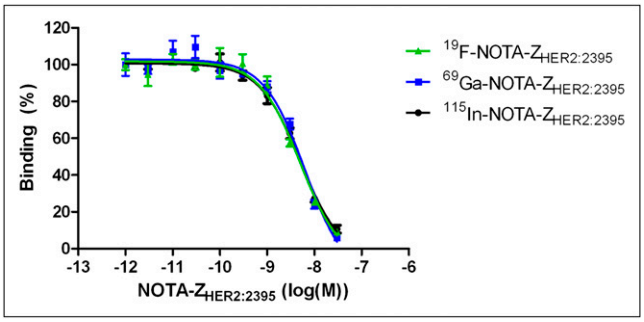

FIGURE 2. Competitive binding curves of IC_{50} determination of ^{19}F-, ^{69}F-, and ^{115}In-NOTA-$Z_{HER2:2395}$ on SK-OV-3 cells. ^{111}In-NOTA-$Z_{HER2:2395}$ was used as radioactive tracer.

beled $Z_{HER2:2395}$. All radiolabeled Affibody molecules showed rapid clearance from the blood and normal organs, resulting in tumor-to-blood ratios of 7.4 ± 1.8 and 8.0 ± 1.3 for ^{18}F- and ^{68}Ga-NOTA-$Z_{HER2:2395}$, respectively (Fig. 4). In contrast, ^{111}In-NOTA-$Z_{HER2:2395}$ cleared from the blood more slowly, resulting in a significantly lower tumor-to-blood ratio of 4.8 ± 1.3 ($P < 0.05$). ^{18}F-NOTA-$Z_{HER2:2395}$ showed good tumor retention: 4 h after injection, tumor uptake was 4.9% ± 0.7 %ID/g, which was comparable to the uptake at 1 h after injection. Tumor uptake of ^{111}In-NOTA-$Z_{HER2:2395}$ was 7.7% ± 2.6 %ID/g at 4 h after injection. Because of faster blood clearance, the tumor-to-blood ratio of ^{18}F-NOTA-$Z_{HER2:2395}$ was significantly higher than that of ^{111}In-NOTA-$Z_{HER2:2395}$ (145 ± 24 vs. 42 ± 13). All 3 radiolabeled Affibody molecules were excreted and reabsorbed by the kidneys, resulting in high kidney accumulation. The bone uptake was low, indicating stable complexation of ^{18}F by the NOTA chelator.

PET/CT and SPECT/CT

PET/CT and SPECT/CT images acquired at 1 and 4 h after injection are shown in Figure 5. ^{18}F-NOTA-$Z_{HER2:2395}$ clearly visualized *HER2*-expressing SK-OV-3 xenografts, with good contrast to normal tissue. ^{68}Ga- and ^{111}In-NOTA-$Z_{HER2:2395}$ also visualized SK-OV-3 xenografts with PET/CT and SPECT/CT, respectively. High accumulation of radiolabeled Affibody molecules in the kidneys was

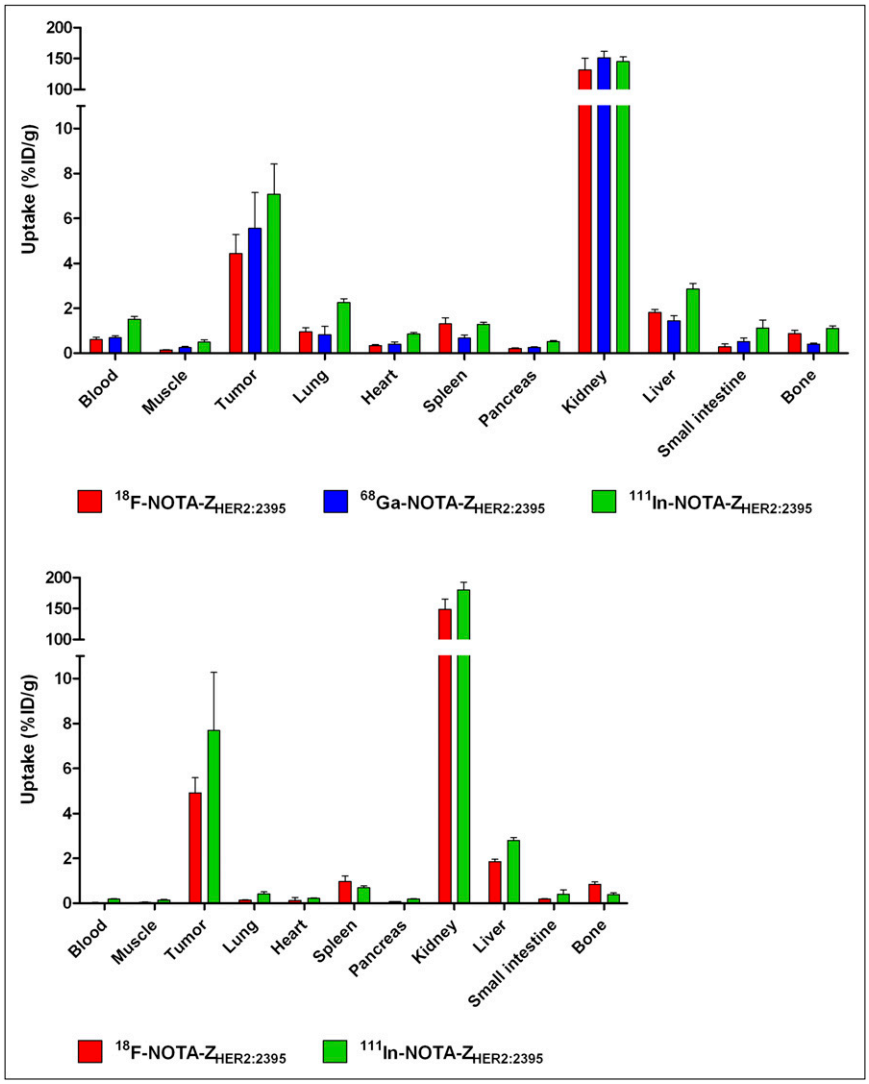

FIGURE 3. Biodistribution of ^{18}F-NOTA-$Z_{HER2:2395}$, ^{68}Ga-NOTA-$Z_{HER2:239}$, and ^{111}In-NOTA-$Z_{HER2:2395}$ in mice bearing subcutaneous SK-OV-3 xenografts at 1 h (A) and 4 h (B) after injection.

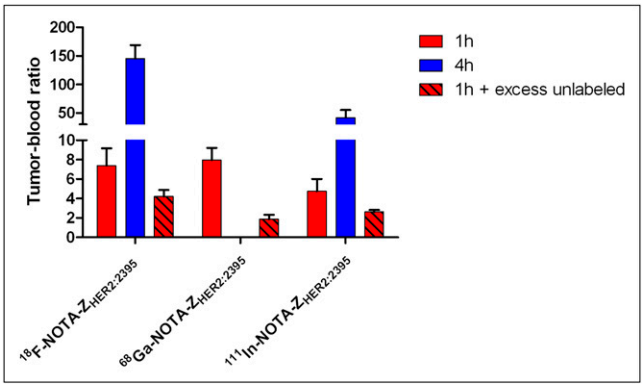

FIGURE 4. Tumor-to-blood ratios of ^{18}F-NOTA-$Z_{HER2:2395}$, ^{68}Ga-NOTA-$Z_{HER2:2395}$, and ^{111}In-NOTA-$Z_{HER2:2395}$ in mice bearing subcutaneous SK-OV-3 xenografts.

observed, with activity mainly localized in the renal cortex. Tumor-to-liver ratios were derived from the PET and SPECT images and ranged between 4.9 and 7.1, 1.6 and 5.3, and 2.6 and 5.8 for ^{18}F-, ^{68}Ga-, and ^{111}In-NOTA-$Z_{HER2:2395}$, respectively. These ratios correlated significantly with the tumor-to-liver ratio measured in the biodistribution study ($r = 0.87$, $P = 0.023$).

DISCUSSION

The preclinical studies described in this paper show that ^{18}F-NOTA-$Z_{HER2:2395}$ is a promising radiotracer for *HER2*-expressing xenografts. This is the first time, to our knowledge, that Affibody molecules were radiolabeled with ^{18}F, based on the complexation of Al^{18}F by NOTA, which is a fast (30 min) labeling reaction. ^{18}F-NOTA-$Z_{HER2:2395}$ has a high affinity for *HER2* ($K_d = 6.5$ nM) and showed efficient and specific accumulation in *HER2*-expressing tumors. PET images revealed high tumor–to–normal tissue contrast.

The in vitro affinity of cold labeled NOTA- $Z_{HER2:2395}$ and the in vivo biodistribution of ^{18}F-NOTA-$Z_{HER2:2395}$ were compared with ^{68}Ga- and ^{111}In-labeled NOTA-$Z_{HER2:2395}$. In vitro, all 3 cold labeled compounds showed similar IC_{50} in the nanomolar range, indicating that the affinity was not affected by the radionuclide that was chelated by NOTA. The comparative biodistribution study showed *HER2*-specific accumulation in the tumor of all radiolabeled Affibody molecules, with the highest tumor uptake for ^{111}In-NOTA-$Z_{HER2:2395}$. However, ^{18}F- and ^{68}Ga-labeled Affibody molecules cleared more rapidly from the blood, resulting in higher tumor-to-blood ratios than ^{111}In-labeled Affibody molecules. Radiolabeled Affibody molecules showed good tumor retention, tumor uptake remained high 4 h after injection, and tumor-to-blood ratios increased rapidly because of the ongoing clearance from the blood. Both PET/CT and SPECT/CT images clearly visualized *HER2*-expressing xenografts, with high contrast to normal tissues. Radiolabeled Affibody molecules were reabsorbed by the kidneys, resulting in high kidney uptake, which was mainly localized in the cortex. PET/CT did not reveal any bone uptake, indicating that the ^{18}F was stably complexed by NOTA.

Overall, all 3 radiolabeled Affibody molecules were able to target and visualize *HER2*-expressing tumors. However, the use of positron-emitting radionuclides such as ^{18}F and ^{68}Ga is preferred over ^{111}In because of the higher sensitivity and better quantification of PET than of SPECT. Moreover, clinical PET/CT cameras have a better resolution than SPECT. An advantage of ^{18}F over ^{68}Ga is the longer half-life (110 vs. 68 min). Therefore, ^{18}F-NOTA-$Z_{HER2:2395}$ allows imaging at several hours after injection, which is preferred because of the higher tumor–to–normal tissue ratios. Moreover, imaging at several hours after injection is practical in the clinical situation. Furthermore, the positron range of ^{18}F (2.3 mm in water) is shorter than that of ^{68}Ga (8.9 mm in water), which can improve image quality, especially in the preclinical setting (*28*).

Several other approaches for imaging of *HER2* expression have been described. $Z_{HER2:342}$ or its derivates have been radiolabeled with different radionuclides and showed specific targeting of *HER2*-expressing xenografts (*17*). Kramer-Marek et al. have conjugated $Z_{HER2:342}$ with ^{18}F-FBEM (*22*). ^{18}F-FBEM-$Z_{HER2:342}$, compared with our ^{18}F-labeled Affibody molecule, was able to bind *HER2* with good affinity and showed comparable uptake in SK-OV-3 xenografts. The specific activities of ^{18}F-NOTA-$Z_{HER2:2395}$ and ^{18}F-FBEM-$Z_{HER2:342}$ were comparable at the end of synthesis. However, the preparation of ^{18}F-FBEM-

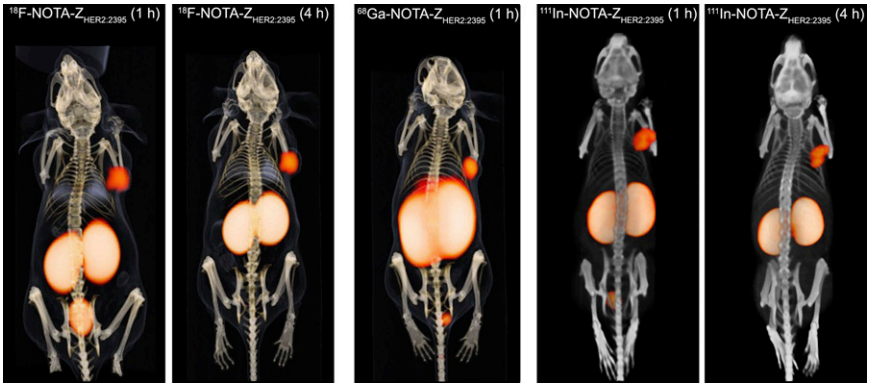

FIGURE 5. PET/CT and SPECT/CT images of mice bearing subcutaneous SK-OV-3 xenografts after injection of radiolabeled NOTA-$Z_{HER2:2395}$.

$Z_{HER2:342}$ is based on the synthesis of a fluorinated synthon, which is subsequently reacted with the Affibody molecule. This process requires a long synthesis time of approximately 2 h. We were able to radiolabel Affibody molecules with ^{18}F within 30 min using a 2-step, 1-pot reaction. In addition, in future studies the specific activity of ^{18}F-NOTA-$Z_{HER2:2395}$ may be improved by using different chelators and solvents (*29,30*).

Besides radiolabeled Affibody molecules, other radiotracers have been developed. For example, radiolabeled trastuzumab and pertuzumab have been used for SPECT and PET of *HER2* expression (*13,14,16,31*). However, these large proteins are characterized by slow tumor penetration and clearance from the circulation. A direct comparison of ^{124}I-labeled $Z_{HER2:342}$ and trastuzumab showed that Affibody molecules have superior imaging properties (*32*). Radiolabeled trastuzumab resulted in higher absolute tumor uptake, but tumor–to–normal tissue ratios were considerably higher for Affibody molecules. Moreover, high-contrast images with Affibody molecules could be obtained within 6 h after injection, in contrast to radiolabeled trastuzumab, for which the highest tumor–to–normal tissue ratios were obtained several days after injection. A disadvantage of trastuzumab-based tracers is that they cannot be used to monitor changes in *HER2* expression during trastuzumab treatment, because of competition of the therapeutic antibody with the tracer molecule for the same epitope on *HER2*. In contrast, in agreement with previously published data (*22*), trastuzumab did not interfere with the binding of NOTA-$Z_{HER2:2395}$ to *HER2*, because of the binding of trastuzumab to different domains. Therefore, Affibody molecules can be used to study *HER2* expression during trastuzumab treatment, which offers exciting opportunities to get more insight into the dynamics of the *HER2* receptor during trastuzumab (combination) therapy.

Translation of *HER2* imaging from the preclinical setting to patients may improve patient selection for *HER2*-targeted therapy, because in vivo imaging avoids misinterpretation due to intratumoral and interlesional tumor heterogeneity. Furthermore, *HER2* imaging can be used to monitor expression during the course of disease or during trastuzumab treatment, without the need of repetitive invasive biopsies. Recently, a clinical pilot study showed that it is feasible to visualize *HER2*-expressing tumors in patients with metastatic breast cancer, using radiolabeled Affibody molecules (*20*).

Despite the advantages of imaging *HER2* expression with Affibody molecules, a few potential limitations have to be considered. First, *HER2*-overexpressing tumors can release *HER2* in the circulation. Circulating *HER2* can bind radiolabeled Affibody molecules and may therefore interfere with tumor targeting. However, a first pilot study showed that *HER2*-overexpressing tumors could be visualized, even in the presence of shed *HER2* (*20*). A second potential limitation is the reabsorption of Affibody molecules by the kidneys, resulting in high kidney accumulation. This may interfere with the visualization of tumor lesions located in the kidney—not a major problem as far as breast and gastric cancers are concerned, because they are not likely to metastasize to the kidneys. Still, there are indications, such as the visualization of lower vertebral lesions, for which *HER2* imaging with ^{18}F-NOTA-$Z_{HER2:2395}$ could be improved by developing strategies to minimize the reabsorption of Affibody molecules by the kidney. Potential ways of reducing kidney uptake are the use of positively charged amino acids, gelofusin, or albumin fragments (*33–35*).

CONCLUSION

This study showed that ^{18}F-NOTA-$Z_{HER2:2395}$ is a promising new imaging agent for *HER2* expression in tumors. Affibody molecules were successfully labeled with ^{18}F within 30 min, based on the complexation of $Al^{18}F$ by NOTA. Further research is needed to determine whether this technique can be used for patient selection for *HER2*-targeted therapy.

DISCLOSURE STATEMENT

The costs of publication of this article were defrayed in part by the payment of page charges. Therefore, and solely to indicate this fact, this article is hereby marked "advertisement" in accordance with 18 USC section 1734.

ACKNOWLEDGMENTS

We thank Bianca Lemmers–de Weem, Kitty Lemmens–Hermans, and Henk Arnts (Central Animal Facility, Radboud University Nijmegen) for technical assistance. This study was financially supported by a personal research grant from the Dutch Research Council (016.096.010) and financial support by the Swedish Cancer Society (Cancerfonden) and the Swedish Research Council (Vetenskapsrådet). The patented AlF labeling method was generously made available by Immunomedics, Inc. (Morris Plains, NJ). No other potential conflict of interest relevant to this article was reported.

REFERENCES

1. Baselga J, Swain SM. Novel anticancer targets: revisiting ERBB2 and discovering ERBB3. *Nat Rev Cancer.* 2009;9:463–475.
2. Meric-Bernstam F, Hung MC. Advances in targeting human epidermal growth factor receptor-2 signaling for cancer therapy. *Clin Cancer Res.* 2006;12:6326–6330.
3. Burstein HJ. The distinctive nature of HER2-positive breast cancers. *N Engl J Med.* 2005;353:1652–1654.
4. Marty M, Cognetti F, Maraninchi D, et al. Randomized phase II trial of the efficacy and safety of trastuzumab combined with docetaxel in patients with human epidermal growth factor receptor 2-positive metastatic breast cancer administered as first-line treatment: the M77001 study group. *J Clin Oncol.* 2005; 23:4265–4274.
5. Slamon DJ, Leyland-Jones B, Shak S, et al. Use of chemotherapy plus a monoclonal antibody against HER2 for metastatic breast cancer that overexpresses HER2. *N Engl J Med.* 2001;344:783–792.
6. Bang YJ, Van CE, Feyereislova A, et al. Trastuzumab in combination with chemotherapy versus chemotherapy alone for treatment of HER2-positive ad-

vanced gastric or gastro-oesophageal junction cancer (ToGA): a phase 3, open-label, randomised controlled trial. *Lancet.* 2010;376:687–697.
7. Geyer CE, Forster J, Lindquist D, et al. Lapatinib plus capecitabine for HER2-positive advanced breast cancer. *N Engl J Med.* 2006;355:2733–2743.
8. Harris L, Fritsche H, Mennel R, et al. American Society of Clinical Oncology 2007 update of recommendations for the use of tumor markers in breast cancer. *J Clin Oncol.* 2007;25:5287–5312.
9. Wolff AC, Hammond ME, Schwartz JN, et al. American Society of Clinical Oncology/College of American Pathologists guideline recommendations for human epidermal growth factor receptor 2 testing in breast cancer. *J Clin Oncol.* 2007;25:118–145.
10. Tuma RS. Inconsistency of HER2 test raises questions. *J Natl Cancer Inst.* 2007; 99:1064–1065.
11. Lower EE, Glass E, Blau R, Harman S. HER-2/neu expression in primary and metastatic breast cancer. *Breast Cancer Res Treat.* 2009;113:301–306.
12. Zidan J, Dashkovsky I, Stayerman C, Basher W, Cozacov C, Hadary A. Comparison of HER-2 overexpression in primary breast cancer and metastatic sites and its effect on biological targeting therapy of metastatic disease. *Br J Cancer.* 2005;93:552–556.
13. Lub-de Hooge MN, Kosterink JG, Perik PJ, et al. Preclinical characterisation of ^{111}In-DTPA-trastuzumab. *Br J Pharmacol.* 2004;143:99–106.
14. Paudyal P, Paudyal B, Hanaoka H, et al. Imaging and biodistribution of Her2/neu expression in non-small cell lung cancer xenografts with Cu-labeled trastuzumab PET. *Cancer Sci.* 2010;101:1045–1050.
15. Tang Y, Wang J, Scollard DA, et al. Imaging of HER2/neu-positive BT-474 human breast cancer xenografts in athymic mice using ^{111}In-trastuzumab (Herceptin) Fab fragments. *Nucl Med Biol.* 2005;32:51–58.
16. McLarty K, Cornelissen B, Cai Z, et al. Micro-SPECT/CT with ^{111}In-DTPA-pertuzumab sensitively detects trastuzumab-mediated HER2 down-regulation and tumor response in athymic mice bearing MDA-MB-361 human breast cancer xenografts. *J Nucl Med.* 2009;50:1340–1348.
17. Löfblom J, Feldwisch J, Tolmachev V, Carlsson J, Stahl S, Frejd FY. Affibody molecules: engineered proteins for therapeutic, diagnostic and biotechnological applications. *FEBS Lett.* 2010;584:2670–2680.
18. Nygren PA. Alternative binding proteins: affibody binding proteins developed from a small three-helix bundle scaffold. *FEBS J.* 2008;275:2668–2676.
19. Tolmachev V, Wallberg H, Sandstrom M, Hansson M, Wennborg A, Orlova A. Optimal specific radioactivity of anti-HER2 Affibody molecules enables discrimination between xenografts with high and low HER2 expression levels. *Eur J Nucl Med Mol Imaging.* 2011;38:531–539.
20. Baum RP, Prasad V, Muller D, et al. Molecular imaging of HER2-expressing malignant tumors in breast cancer patients using synthetic ^{111}In- or ^{68}Ga-labeled affibody molecules. *J Nucl Med.* 2010;51:892–897.
21. Tolmachev V, Altai M, Sandstrom M, et al. Evaluation of a maleimido derivative of NOTA for site-specific labeling of Affibody molecules. *Bioconjug Chem.* 2011;22:894–902.
22. Kramer-Marek G, Kiesewetter DO, Martiniova L, Jagoda E, Lee SB, Capala J. [^{18}F]FBEM-$Z_{HER2:342}$-Affibody molecule-a new molecular tracer for in vivo monitoring of HER2 expression by positron emission tomography. *Eur J Nucl Med Mol Imaging.* 2008;35:1008–1018.
23. McBride WJ, Sharkey RM, Karacay H, et al. A novel method of ^{18}F radiolabeling for PET. *J Nucl Med.* 2009;50:991–998.
24. Laverman P, McBride WJ, Sharkey RM, et al. A novel facile method of labeling octreotide with ^{18}F-fluorine. *J Nucl Med.* 2010;51:454–461.
25. Ahlgren S, Orlova A, Rosik D, et al. Evaluation of maleimide derivative of DOTA for site-specific labeling of recombinant affibody molecules. *Bioconjug Chem.* 2008;19:235–243.
26. Visser EP, Disselhorst JA, Brom M, et al. Spatial resolution and sensitivity of the Inveon small-animal PET scanner. *J Nucl Med.* 2009;50:139–147.
27. van der Have F, Vastenhouw B, Ramakers RM, et al. U-SPECT-II: an ultra-high-resolution device for molecular small-animal imaging. *J Nucl Med.* 2009;50: 599–605.
28. Disselhorst JA, Brom M, Laverman P, et al. Image-quality assessment for several positron emitters using the NEMA NU 4-2008 standards in the Siemens Inveon small-animal PET scanner. *J Nucl Med.* 2010;51:610–617.
29. D'Souza CA, McBride WJ, Sharkey RM, Todaro LJ, Goldenberg DM. High-yielding aqueous ^{18}F-labeling of peptides via Al^{18}F chelation. *Bioconjug Chem.* 2011;22:1793–1803.
30. McBride WJ, D'Souza CA, Sharkey RM, et al. Improved ^{18}F labeling of peptides with a fluoride-aluminum-chelate complex. *Bioconjug Chem.* 2010;21:1331–1340.
31. Dijkers EC, Kosterink JG, Rademaker AP, et al. Development and characterization of clinical-grade ^{89}Zr-trastuzumab for HER2/neu immunoPET imaging. *J Nucl Med.* 2009;50:974–981.
32. Orlova A, Wallberg H, Stone-Elander S, Tolmachev V. On the selection of a tracer for PET imaging of HER2-expressing tumors: direct comparison of a ^{124}I-labeled affibody molecule and trastuzumab in a murine xenograft model. *J Nucl Med.* 2009;50:417–425.
33. Rolleman EJ, Valkema R. de JM, Kooij PP, Krenning EP. Safe and effective inhibition of renal uptake of radiolabelled octreotide by a combination of lysine and arginine. *Eur J Nucl Med Mol Imaging.* 2003;30:9–15.
34. van Eerd JE, Vegt E, Wetzels JF, et al. Gelatin-based plasma expander effectively reduces renal uptake of ^{111}In-octreotide in mice and rats. *J Nucl Med.* 2006;47: 528–533.
35. Vegt E, van Eerd JE, Eek A, et al. Reducing renal uptake of radiolabeled peptides using albumin fragments. *J Nucl Med.* 2008;49:1506–1511.